IRT DATE	3. REPORT TYPE AND DATES COVERED
5/29/92	Technical

4. TITLE AND SUBTITLE

Photodynamics within $\{CH_3OH\}_nCr(CO)_6$ Heteroclusters: Observation of an Isotope Effect

5. FUNDING NUMBERS

R & T Code:
413n008

G N00014-88-K-0483

6. AUTHOR(S)

William R. Peifer and James F. Garvey

7. PERFORMING ORGANIZATION NAME(S) AND ADDRESS(ES)

Dept. of Chemistry, Acheson Hall
State University of New York at Buffalo
Buffalo, NY
14214

8. PERFORMING ORGANIZATION REPORT NUMBER

Technical Report #26

9. SPONSORING/MONITORING AGENCY NAME(S) AND ADDRESS(ES)

Dr. R. DeMarco/Dr. J. Pazik, Chemistry Division
Office of Naval Research
800 N. Quincy St.
Arlington, VA
22217

10. SPONSORING/MONITORING AGENCY REPORT NUMBER

11. SUPPLEMENTARY NOTES

12a. DISTRIBUTION/AVAILABILITY STATEMENT

Approved for public release;
distribution unlimited

12b. DISTRIBUTION CODE

13. ABSTRACT *(Maximum 200 words)*

We have recently examined the multiphoton dissociation and ionization dynamics of mixed van der Waals heteroclusters of $Cr(CO)_6$ solvated by methanol, and have inferred from photoion fragmentation branching ratios that CD_3OD is more efficient than CH_3OH in relaxing excess internal energy of the nascent photoion via intracluster energy transfer. Multiphoton ionization is suggested to proceed via single-photon photodissociation of the solvated $Cr(CO)_6$, followed by two-photon ionization of the coordinatively unsaturated photoproduct. Excess energy in the internal modes of the nascent photoion appears to be disposed of via non-statistical, mode-specific transfer to the internal degrees of freedom of an adjacent solvent molecule within the cluster. Photoionization using laser power densities on the order of 10^{12} to 10^{13} W/cm^2 is accompanied by extensive intracluster bimolecular chemistry.

14. SUBJECT TERMS

15. NUMBER OF PAGES

16. PRICE CODE

17. SECURITY CLASSIFICATION OF REPORT	18. SECURITY CLASSIFICATION OF THIS PAGE	19. SECURITY CLASSIFICATION OF ABSTRACT	20. LIMITATION OF ABSTRACT
UNCLASSIFIED	UNCLASSIFIED	UNCLASSIFIED	UL

OFFICE OF NAVAL RESEARCH

GRANT N00014-88-K-0483

R & T Code 413n008

Technical Report No. 26

Photodynamics within $\{CH_3OH\}_nCr(CO)_6$ Heteroclusters: Observation of an Isotope Effect

by

William R. Peifer and James F. Garvey*

Prepared for Publication
in
Isotope Effect in Chemical Reaction and Photodissociation Processes, edited by
Jack A. Kaye, A.C.S. Books, Washington, DC

Acheson Hall
Department of Chemistry
University at Buffalo
The State University of New York at Buffalo
Buffalo, NY
14214

June 1, 1992

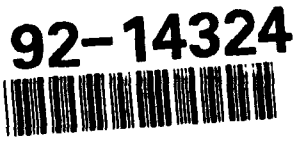

Multiphoton Ionization Dynamics Within $(CH_3OH)_nCr(CO)_6$ van der Waals Clusters: Isotope Effects in Intracluster Energy Transfer

William R. Peifer and James F. Garvey*

Acheson Hall
Department of Chemistry
State University of New York at Buffalo
Buffalo, New York 14214

We have recently examined the multiphoton dissociation and ionization dynamics of mixed van der Waals heteroclusters of $Cr(CO)_6$ solvated by methanol, and have inferred from photoion fragmentation branching ratios that CD_3OD is more efficient than CH_3OH in relaxing excess internal energy of the nascent photoion via intracluster energy transfer. Multiphoton ionization is suggested to proceed via single-photon photodissociation of the solvated $Cr(CO)_6$, followed by two-photon ionization of the coordinatively unsaturated photoproduct. Excess energy in the internal modes of the nascent photoion appears to be disposed of via non-statistical, mode-specific transfer to the internal degrees of freedom of an adjacent solvent molecule within the cluster. Photoionization using laser power densities on the order of 10^{12} to 10^{13} W/cm^2 is accompanied by extensive intracluster bimolecular chemistry.

Perhaps one of the most fundamental of challenges at the interface of physics and chemistry is the unraveling of the detailed sequence of events which ensues when two molecules collide (*1*). For a macroscopic system composed of many molecules, one may observe the phenomenological consequences of a very large number of collisions averaged over time, energy, and collision geometry. The chemical dynamicist, who wishes to study individual collisions, may start with a prior knowledge of the chemical identities of reactants and products, and attempt to probe the influence of reactant quantum state and geometry of approach on reaction probability, as well as the redistribution of available energy amongst the various degrees of freedom throughout the encounter. Indeed, reasonably complete ab initio treatment of some of the simpler atom transfer reactions is currently within the realm of computational tractability (*2*), and the experimental study of more complicated systems will no doubt provide a stringent proving ground for the refinement of quantum theoretical approaches.

Given a sufficiently detailed understanding of the collision dynamics for a particular set of reactants, one could in principle deduce the behavior and properties of a macroscopic ensemble of reactant molecules in the condensed phase (*3*). Unfortunately, our understanding of the dynamics for even the simplest of systems is generally not of sufficient detail to permit such an a priori deduction. If we wish to bring the power of a chemical dynamics approach to bear upon the study of chemistry within condensed phases, thereby shedding light on the evolution of physical and chemical properties from those of isolated pairs of molecules undergoing collision to those of macroscopic collections of such molecules, we must develop appropriate models for experimental inquiry.

An emergent sub-discipline of physical chemistry directed toward the development and study of such models is the field of van der Waals cluster research (*4*). The study of bimolecular chemistry within these van der Waals clusters provides a conceptual link between bimolecular reaction dynamics in the gas phase, and processes of equal or higher molecularity in condensed phases. Clusters of a few to several hundred molecules may be easily generated in the free-jet expansions of molecular beams, and subsequently interrogated by a variety of powerful laser spectroscopic and mass spectrometric techniques. These clusters are sufficiently small to be amenable to theoretical treatment, yet sufficiently large to serve as sophisticated models for the study of such condensed-phase phenomena as aerosol formation, crystallization, and structural and mechanistic aspects of solvation. Intracluster bimolecular chemistry may be induced through the creation of reactive species within clusters via electron impact, optical excitation, or photodissociation of appropriate precursor molecules. The experimentalist has control over not only the internal energies of these cluster-bound reactants, but in many cases the collision geometry as well, since the arrangement of molecules within van der Waals clusters is often highly ordered (*5,6*).

A matter of considerable interest to the cluster research community involves energy disposal processes within van der Waals clusters (*7*). How does a cluster in which an exothermic bimolecular reaction has just taken place dispose of the excess energy? How is the internal energy which is localized on a single molecule, perhaps even in a single vibrational or rotational mode, transferred to the remaining molecules within the cluster, and on what timescale does such intracluster energy redistribution take place? How well can the cluster accommodate this redistributed energy, and by what mechanisms does the entire cluster ultimately dissipate that portion of redistributed energy which cannot be accommodated? It has been well-established from the study of the fragmentation of cluster ions, following electron impact excitation of size-selected neutral clusters, that an important and general energy disposal mechanism is the sequential ejection, or evaporation, of individual molecules from the cluster. This process is accurately modeled by Boltzmann statistics and can be likened to the macroscopic process of evaporative cooling in liquids and solids. Alternatively, one may view this process within the microscopic context of chemical dynamics, wherein the relaxation

of excess energy in the electronic, vibrational, and/or rotational degrees of freedom of a given molecule within the cluster, correlates ultimately with the appearance of excess energy in the translational degrees of freedom of the remaining molecules: such processes can be referred to as *E-T*, *V-T*, or *R-T* energy transfer.

Does the relaxation of any given excited molecule within a van der Waals cluster always proceed by means of a purely statistical transfer of energy to translations of the surrounding molecules? Recent experiments within our own research group suggest that this is not always the case; that, in fact, excitation in the internal modes of a given molecule can in some cases be transferred preferentially to a restricted number of modes in the surrounding molecules (for example, to a specific bending or stretching motion of the acceptor molecule). We have recently examined the multiphoton dissociation and ionization dynamics of $Cr(CO)_6$ bound within van der Waals clusters of either CH_3OH or CD_3OD (*8,9*). In addition to uncovering some rather unusual photophysics, we have gained some insight regarding the mode-specific character of intracluster energy transfer processes occurring between excited photoproducts of $Cr(CO)_6$ and the surrounding "solvent" molecules. In this chapter, we review our study of the multiphoton ionization dynamics for two systems of heterogeneous van der Waals clusters: $(CH_3OH)_nCr(CO)_6$, and the perdeuterated isotopomers, $(CD_3OD)_nCr(CO)_6$. We discuss differences in the observed photofragment cluster ion yields, and their implications for intracluster energy transfer and relaxation processes.

Rationale for Selection of the Model Heterocluster Systems

Of the myriad intracluster energy transfer processes which one might choose to examine, we have undertaken a study of energy transfer from excited $Cr(CO)_6$ photoproducts to surrounding solvent molecules of either CH_3OH or CD_3OD. Our motivation for the selection of these particular systems stems from fundamental interests in three principal areas: namely, the single- and multiple-photon photochemistry of coordinatively saturated transition metal carbonyls, the chemical significance of coordinatively unsaturated metal carbonyls in stoichiometric and catalytic reactions, and the development of techniques for spectroscopic characterization of these reactive, unsaturated species.

Photophysics of Transition Metal Carbonyls. Coordinatively unsaturated transition metal carbonyls play a central role in mechanistic organometallic chemistry (*10*). Many of these species are thought to be important intermediates in industrially significant catalytic schemes (*11,12*). These highly reactive molecules can be conveniently synthesized in the laboratory by pulsed UV laser photolysis of coordinatively saturated precursors (*13*). In condensed phases, absorption of a single UV photon by the precursor molecule results in the loss of a single ligand, independent of photon

wavelength (*14*), and sequential absorption of several photons is likewise accompanied by sequential loss of additional ligands. In the gas phase, the extent of ligand loss is highly wavelength-dependent, and single-photon absorption may lead to multiple-ligand loss (*15-17*). Absorption of multiple photons by isolated metal carbonyl molecules in the gas phase results primarily in complete ligand stripping, or multiphoton dissociation (MPD), rather than molecular ionization. (Such photophysical behavior is typical of organometallic compounds in general.) Consequently, atomic metal ions are often the only photoproduct ions observed following multiphoton ionization (MPI) of organometallic compounds (*18*). To understand this transition in photophysical behavior from that typical of isolated molecules in the gas phase to that of solvated molecules in condensed phases, we need to develop an understanding of energy transfer processes between internally excited metal carbonyls and adjacent molecules in the surrounding environment.

Spectroscopic Probes of Relaxation Dynamics in Metal Carbonyls. A variety of spectroscopic techniques have been utilized by several groups to examine the relaxation dynamics of the excited species produced following UV photolysis of transition metal carbonyls in both the gas phase and condensed phases. Weitz and co-workers (*19-22*), Rosenfeld and co-workers (*23-25*), and Rayner and co-workers (*26*) have employed a transient infrared absorption technique to probe the photolysis of Group VIB hexacarbonyls in the gas phase. From these studies have come a wealth of information on the vibrational spectra, geometry, metal-ligand bond strengths, reactivity, and vibrational relaxation rates for various unsaturated metal carbonyls in their electronic ground states. The dynamics of UV photolysis of $Cr(CO)_6$ in the liquid phase, as well as the solvation dynamics for the nascent $Cr(CO)_5$ photoproduct, have been studied on the picosecond and sub-picosecond timescales in the transient visible absorption experiments of Nelson (*27*), Lee and Harris (*28*), and Simon and Xie (*29-32*); the transient IR absorption experiments of Spears and co-workers (*33,34*) and Hochstrasser and co-workers (*35*); and the transient Raman scattering experiments of Hopkins and co-workers (*36*). From these studies, we have developed an understanding of the microscopic details of the solvation process and the timescale for vibrational relaxation of $Cr(CO)_5$ in its electronic ground state following solvation.

The spectroscopic pump-probe techniques described above are all suitable for studying vibrational relaxation of metal carbonyls in the ground electronic state. Relaxation of excited electronic states in solution occurs on a timescale too rapid to probe, even with the <100-femtosecond timescale (*27*) of the fastest transient visible absorption technique. Upper electronic states of naked (isolated, gas-phase) metal carbonyls are difficult to study directly, using conventional UV laser absorption and emission techniques, since excited states of these species generally undergo rapid and efficient internal conversion to repulsive surfaces. UV absorption bands are consequently broad and quite diffuse. If we hope to advance our understanding of the upper elec-

tronic structure of metal carbonyls, relaxation dynamics of molecules in these excited states, and the significance of electronic excitation in mechanistic organometallic chemistry, we need to develop gas-phase spectroscopic probes of organometallic electronic structure.

MPI of van der Waals Clusters Containing $M(CO)_6$ (M = Cr, Mo, W). Very early in the course of our own studies of the photophysics and photochemistry of organometallic species within van der Waals clusters, we discovered that MPI, combined with mass spectrometry, might in fact be a suitable probe of the intracluster bimolecular reactivity (if not the electronic spectroscopy) of coordinatively unsaturated Group VIB carbonyls. We observed that the photoproduct ions following 248-nm MPI of homogeneous van der Waals clusters of either $Mo(CO)_6$ or $W(CO)_6$ are not exclusively atomic metal ions, as one might expect by analogy with the photophysics of the naked hexacarbonyls, but include a significant yield of totally unexpected metal oxide ions as well (*37,38*). These photoions could not be attributed to reactions of $M(CO)_6$ photoproducts with oxygen containing impurities (e.g., H_2O, O_2, etc.) present in the molecular beam. Since we did not observe these metal oxide ions in the electron impact cluster mass spectrum, we reasoned that the metal oxide ions were not the products of an intracluster ion-molecule reaction.

We suggested that these metal oxide ions were instead daughter ions which arise following photoionization of the binuclear product of some reaction between a neutral coordinatively unsaturated metal carbonyl and an adjacent hexacarbonyl "solvent" molecule within the cluster. This type of neutral bimolecular chemistry is analogous to that which takes place in the gas phase, generally at or near gas-kinetic rates for spin-allowed reactions, between unclustered partners (*39*). We considered the mechanistic implications of our unusual observations, borrowing from insights in molecular orbital theory, synthetic organometallic chemistry, and surface science, and predicted that the inferred intracluster chemistry would take place for coordination compounds of metals with large d-orbitals (such as Mo and W), but not for those of metals with more contracted d-orbitals (such as Cr). This prediction was, in fact, borne out as we failed to observe evidence of the analogous chemistry following MPI of $Cr(CO)_6$ van der Waals clusters.

To further understand the unusual photophysics of these van der Waals clusters of Group VIB hexacarbonyls, and to unravel the intracluster chemistry, we decided that we needed to examine the MPD and MPI of these molecules within clusters of more inert "solvent" molecules. We chose $Cr(CO)_6$, since the photophysics for naked $Cr(CO)_6$ has been studied in greater depth and is better-characterized than those of the other two hexacarbonyls. We chose methanol as a solvent molecule for several reasons. First, it possesses a vapor pressure and ionization potential which are both conveniently high (making it possible to generate fairly large heteroclusters whose solvent molecules are not easily ionized). Second, it is a moderate σ-donor and a poor π-ac-

ceptor, so we would not expect significant perturbations of the ligand field states due to the proximity of methanol molecules within the clusters. Finally, vibronic relaxation of $Cr(CO)_5$ by liquid-phase methanol has been extensively studied (*27-29,36*). We describe in the remainder of this chapter our most recent research involving the MPI of $Cr(CO)_6$-containing heteroclusters.

Time-of-flight Mass Spectrometry of $Cr(CO)_6$-containing Heteroclusters Following Multiphoton Ionization

Experimental Apparatus. A detailed description of the experimental apparatus and protocol has appeared elsewhere (*9*), so we shall give only a brief description here. Heterogeneous van der Waals clusters containing $Cr(CO)_6$ and methanol were produced in the free-jet expansion of a pulsed beam of seeded helium. The resulting cluster beam was skimmed and admitted into the differentially pumped ion source of a commercially-available time-of-flight mass spectrometer (R.M. Jordan Company). The cluster beam was irradiated within the ion source by the output from a pulsed UV laser, which was triggered to fire so that molecules within the center of the molecular beam pulse were photoionized. These photoions were then extracted in a direction perpendicular to both the molecular beam and the laser beam and accelerated to a nominal kinetic energy of about 4 keV. Ions which completed successful trajectories through the 1.5-m flight tube were detected by a dual microchannel plate detector. Mass spectra were collected by irradiating the neutral beam at a constant laser wavelength while acquiring and averaging detector signals following each shot with a digital storage oscilloscope (LeCroy 9400). Optical (MPI) spectra were collected by slowly scanning the wavelength of the pulsed UV laser while using a gated integrator (EG&G/PAR 4420) to acquire and average signal from ions of a given m/z.

Immediately after passing out of the ion source and into the flight tube, the photoions experience a small electric field, normal to the ion beam axis, which is of sufficient magnitude to compensate for any transverse component of photoion kinetic energy. Since neutrals in the molecular beam have the same *forward* component of mean velocity, photoions in the ion beam will have the same *transverse* component of mean velocity (assuming photofragment recoil, if any, is negligible). Consequently, larger cluster photoions will have higher transverse kinetic energy and will reach the detector only if a transverse deflecting field of greater magnitude is employed. The mass spectrometer therefore acts as a crude bandpass filter, efficiently transmitting a narrow range of ions centered about an optimum m/z value which is directly proportional to the magnitude of the deflecting field. A noteworthy point is that ions of smaller-than-optimal m/z may be efficiently transmitted if they have a larger-than-nominal transverse velocity (due, for example, to photofragment recoil in the direction of the neutral beam). Likewise, larger-than-optimal ions with smaller-than-nominal transverse velocity (due, for example, to photofragment recoil in the direction opposite the neutral

beam) may also reach the detector.

Photoionization Lasers. The MPI of $Cr(CO)_6$-containing heteroclusters was examined in two different regions of the UV spectrum. Two distinct laser systems were used as photoionization sources. The first was an excimer laser (Lambda Pysik EMG-150) we operated on the KrF transition at 248 nm. This wavelength is very close to the absorption maximum of $Cr(CO)_6$ assigned as the $^1A_{1g}$ --> $^1T_{1u}$ MLCT band (*40*). $Cr(CO)_4$ is the primary photoproduct of the 248-nm single-photon photodissociation of naked $Cr(CO)_6$ in the gas phase (*41*). Copious photoion yields can be realized following irradiation at this wavelength even with mildly focused laser light (corresponding to power densities on the order of 10^7 W/cm^2).

The second laser we utilized as a photoionization source was an excimer-pumped dye laser (Lambda Physik FL3002) operated with 2-methyl-5-t-butyl-quaterphenyl dye in the range of 346-377 nm. This is near the less-intense $^1A_{1g} \rightarrow {}^1T_{1g}$ LF band of $Cr(CO)_6$ (*40*). $Cr(CO)_5$ is the primary photoproduct of single-photon photodissociation of naked, gas-phase $Cr(CO)_6$ at wavelengths within this range (*42*). An excimer laser operating on the XeF transition at 351 nm accesses the same portion of the UV spectrum. However, we chose to use the dye laser as the second system for two reasons. First, it is necessary to use strongly focused laser light (power densities on the order of 10^{12} to 10^{13} W/cm^2) to produce reasonable photoion yields in this wavelength region, and because of the differing beam divergences of the two lasers, it is possible to get nearly as large of power densities from the tightly focused dye laser as from the tightly focused XeF excimer laser. Second, the tunability of the dye laser allows us to collect resonance enhanced MPI (REMPI) spectra, which give us optical signatures of the neutral species undergoing ionization.

Photoion Yields

Mass Spectra Following MPI at 248 nm. Portions of the mass spectra collected following 248-nm irradiation of $Cr(CO)_6/CH_3OH$ and $Cr(CO)_6/CD_3OD$ cluster beams at moderate power density (10^7 W/cm^2) are shown in Figures 1 and 2, respectively. One immediately notices that the mass spectra are not dominated by signals due to solvated metal ions, as one might expect by analogy with the multiphoton dissociation and ionization dynamics of naked, unclustered $Cr(CO)_6$. Instead, repetitive sequences of solvated molecular ions appear, corresponding to several different chromium carbonyl species in varying states of coordinative unsaturation.Somewhat more careful examination reveals that the sequences of photoions which appear following multiphoton ionization of $Cr(CO)_6/CH_3OH$ heteroclusters are not identical to those which appear following MPI of the perdeuterated isotopomers. While photoionization of the CH_3OH-solvated heteroclusters leads to sequences of empirical formula

$(CH_3OH)_nCr(CO)_x^+$, x=0,1,2,5, and 6 (but not 3), photoionization of the perdeuterated heteroclusters leads to sequences of empirical formula $(CD_3OD)_nCr(CO)_x^+$, where x takes on the values 0,1,2,3, and 6 (but not 5).

Following 248-nm MPI at extremely high power density (10^{13} W/cm^2), the extent of fragmentation increases, as one might expect. As seen in the mass spectra in Figures 3a and 3b, photoions corresponding to solvated $Cr(CO)_x^+$, where x now takes on the values 0,1, and 2, are observed following MPI at high power density. Under these conditions, the same sequences appear following photoionization of either the CH_3OH- or CD_3OD-solvated heteroclusters. However, the branching ratios are now significantly different, with photoionization of the CD_3OD-solvated heteroclusters favoring production of larger proportions of the more extensively ligated species. A prominent sequence of peaks corresponding to $(CH_3OH)_nCr(H_2O)^+$ also appears in the spectrum in Figure 3a. These ions arise not from the presence of trace impurities of water in the gas mixture, but apparently via an intracluster bimolecular reaction, mediated perhaps by the presence of a coordinatively unsaturated chromium carbonyl species within the cluster. The corresponding sequence in the mass spectrum of the perdeuterated heteroclusters is obscured by isobaric interference.

Assuming the identities of the primary photoions do not depend on the identity of the solvent, these observed differences in the mass spectra of the isotopomeric heteroclusters suggest that the rates for relaxation of the nascent parent ions by the surrounding solvent bath, and therefore probabilities for fragmentation to daughter ions, are dependent on solvent identity. Since CH_3OH and CD_3OD are expected to have virtually identical cross sections for collision with a given metal carbonyl ion, it seems unlikely that the intracluster relaxation of the nascent parent ions occurs by a purely statistical process of collisional transfer to translational modes of the solvent bath. Based on our observations, it seems more reasonable that intracluster relaxation of the nascent photoions occurs through the transfer of energy to specific internal modes, perhaps a restricted set of vibrations and/or rotations, of the surrounding solvent molecules. We will discuss this apparent dynamical effect in greater detail after first considering the photoion yields following MPI at other wavelengths.

Mass Spectra Following MPI at 350 nm. The mass spectrum collected following 350-nm MPI of $Cr(CO)_6/CH_3OH$ heteroclusters at extremely high power density (10^{12} W/cm^2) is shown in Figure 4a, and an expanded portion of this spectrum appears in Figure 4b. Features in the mass spectrum are attributed to three sequences of cluster photoions: $(CH_3OH)_nCr(CO)_4H^+$, $(CH_3OH)_nCr(CO)_5H^+$, and $(CH_3OH)_n(H_2O)Cr(CO)_5H^+$. (The $Cr(CO)_5$ moiety is isobaric with the methanol pentamer; however, our assignment was confirmed by comparison with the mass spectrum of the perdeuterated heteroclusters.) Ion trajectory calculations suggest that the ensemble of cluster ions in the spectrum of Figure 4a which is centered around 460

amu corresponds to cluster ions with zero photofragment recoil kinetic energy, while those centered at 260 amu and at 690 amu correspond to ions with recoil vectors of about 1.7 eV in magnitude, oriented either parallel or antiparallel to the molecular beam vector.

The mass spectrum collected following 350-nm MPI of $Cr(CO)_6/CD_3OD$ heteroclusters at extremely high power density (10^{12} W/cm^2) is shown in Figure 5a, and an expansion of this spectrum is shown in Figure 5b. At 350 nm, the contribution to the photoion yield from homogeneous solvent cluster ions is negligible. In this spectrum, sequences of ions assigned as $(CD_3OD)_nCr(CO)_5D^+$ and $(CD_3OD)_n(D_2O)Cr(CO)_5D^+$ are present, but the sequence corresponding to $(CD_3OD)_nCr(CO)_4D^+$ is missing. Again, the fragmentation of the nascent parent ions appears to occur to a lesser extent when they are surrounded by CD_3OD, and to a greater extent when they are surrounded by CH_3OH. There is no evidence of photoions in this mass spectrum with non-negligible photofragment recoil, as was the case with the non-deuterated heteroclusters. As shown in Figure 5c, irradiation at 360 nm (the wavelength of maximum lasing efficiency for the dye) leads primarily to ionization of the homogeneous solvent clusters, while heterocluster photoion yields have dropped by nearly an order of magnitude (relative to yields following irradiation at 350 nm).

Mass-resolved REMPI Spectra: 346-377 nm. Optical spectra collected by plotting yields for $Cr(CO)_5D^+$ (a representative heterocluster photoion), Cr^+, and $(CH_3OH)_7H^+$ (a representative homogeneous solvent cluster photoion) against MPI laser wavelength are shown in Figures 6a, 6b, and 6c, respectively. These REMPI spectra are not corrected for the wavelength dependence of the laser pulse energy, which is shown in Figure 6d. Mass-resolved REMPI spectra provide optical signatures of the neutral species which, upon undergoing MPI, give rise to the monitored photoions. The fact that the heterocluster photoion spectrum does not display the same features as either the Cr^+ spectrum or the solvent cluster ion spectrum can be taken as definitive evidence that the heterocluster ion does not arise from photoionization of either methanol or atomic chromium, but rather some other neutral molecule, presumably a cluster-bound chromium carbonyl species.

Mass spectral evidence strongly suggests that the heterocluster photoions observed following irradiation at 248 nm also arise from MPI of some chromium carbonyl species. Do the heterocluster photoions which appear following 248-nm MPD/MPI, and heterocluster photoions which appear following 350-nm MPD/MPI, arise from ionization of the same neutral precursor? Suppose for the moment that this is, in fact, the case. How would we expect the heterocluster mass spectra following MPI at two different wavelengths to compare?

$Cr(CO)_6$ has a much larger absorption cross section at 248 nm than at 350 nm, and one would expect that under conditions where transitions are not saturated, pho-

tcion yields following MPI at 248 nm would be larger, and the extent of ion photofragmentation would be greater. Under such circumstances, the 248-nm mass spectrum would not be expected to resemble the 350-nm mass spectrum. However, under conditions of sufficiently high power densities (such as the 10^{12} to 10^{13} W/cm^2 used in our high-intensity MPI experiments) essentially all one-photon processes, and many two-photon processes, are expected to be saturated. The extent of ionization and fragmentation should therefore depend not on the energy of the individual photons employed, but on the total number of phctons absorbed by a given molecule. Extensive fragmentation would be expected at any laser wavelength employed, and photofragment branching ratios would be fairly insensitive to laser wavelength. This is typical for MPI of many polyatomic organic molecules, such as benzene, for example (*43*). We have suggested that our 248-nm, high-fluence MPI mass spectrum does not resemble the 350-nm, high-fluence spectrum because the primary photoproduct ion at 248 nm is not the same as the primary photoproduct ion at 350 nm. This would most likely be the case if the neutral chromium carbonyl species undergoing MPI at 248 nm were different from the one undergoing MPI at 350 nm. Furthermore, we can explain not only the photofragment branching ratios, but also the apparent solvent-dependent relaxation phenomenon, if we assume that photodissociation along the neutral ladder, prior to MPI, is analogous to the single-photon photophysics of $Cr(CO)_6$.

Photodissociation and Ionization Dynamics of Cluster-bound $Cr(CO)_6$

Dynamical Scheme. The results of our high-fluence MPI mass spectrometric experiments suggest that the solvated neutral chromium carbonyl species which we are probing via MPI at 248 nm is not identical to the neutral species which we are probing via MPI at 346-377 nm. It seems quite likely, then, that we are spectroscopically probing, via MPI, the neutral products of one-photon photodissociation of cluster-bound $Cr(CO)_6$, and that the coordinatively unsaturated species we are preparing depends on the wavelength we utilize. A not unreasonable extrapolation from the known photophysics of naked $Cr(CO)_6$ in the gas phase suggests a dynamical scheme for the photophysics of cluster dissociation and ionization which is also consistent with the apparent intracluster relaxation processes evidenced in the mass spectra.

The 248-nm photodissociation of naked $Cr(CO)_6$ is known to give rise to an excited photoproduct, $Cr(CO)_4$*, whose internal energy is estimated to be as much as 38 kcal/mol; while the 351-nm photodissociation is known to give rise to a $Cr(CO)_5$* photoproduct, whose internal energy is estimated between 30 and 45 kcal/mol (*42*). The ionization potentials for the ground states of these primary photoproducts can be estimated from known bond dissociation energies and ion appearance potentials, and we have estimated the ionization potentials for naked $Cr(CO)_4$ and $Cr(CO)_5$ to be approximately 167 and 173 kcal/mol, respectively (*9*). Let us take the photophysical de-

$Cr(CO)_4$ and $Cr(CO)_5$ to be approximately 167 and 173 kcal/mol, respectively (9). Let us take the photophysical description of naked $Cr(CO)_6$ and the thermochemical description of the coordinatively unsaturated photoproducts to be appropriate for the description of the cluster-bound analogs. We can then propose the schemes shown below to account for photodissociation, MPI, and subsequent fragmentation.

<u>248 nm</u>

$$S_nCr(CO)_6 + h\upsilon \rightarrow S_nCr(CO)_4^* + 2\,CO$$
$$S_nCr(CO)_4^* + 2h\upsilon \rightarrow [S_nCr(CO)_4^*]^+ \rightarrow [S_{n-1}\cdots S^*\cdots Cr(CO)_4]^+$$
$$[S_nCr(CO)_4^*]^+ \rightarrow [S_nCr(CO)_x]^+ + 4\text{-}x\,CO$$

<u>350 nm</u>

$$S_nCr(CO)_6 + h\upsilon \rightarrow S_nCr(CO)_5^* + CO$$
$$S_nCr(CO)_5^* + 2h\upsilon \rightarrow [S_nCr(CO)_5^*]^+ \rightarrow [S_{n-1}\cdots S^*\cdots Cr(CO)_5]^+$$
$$[S_nCr(CO)_5^*]^+ \rightarrow [S_nCr(CO)_4]^+ + CO$$

In the initial step of each scheme, single-photon absorption by the cluster-bound $Cr(CO)_6$ leads to photodissociation and loss of one or more carbonyl ligands. Subsequent two-photon absorption leads to ionization of the single-photon photoproduct and production of a nascent photoion with a certain degree of excess energy. Assuming the estimated I.P.'s given above for the unsaturated chromium carbonyls are accurate, internal energy for the nascent cluster-bound $[Cr(CO)_4^*]^+$, created via 248-nm MPI, is expected to be as large as 103 kcal/mol. An ion with this much internal energy would be expected to undergo facile loss of additional ligands, giving rise to ions such as the ones we observe following 248-nm MPI. Tyndall and Jackson have observed that low-energy electron impact of the nascent neutral $Cr(CO)_4$ photoproduct resulting from 248-nm photodissociation of $Cr(CO)_6$ results in the production of ions of the formula, $Cr(CO)_x^+$ (x=0,1,2), which have undergone extensive fragmentation (44). Two-photon ionization of the $Cr(CO)_5^*$ photoproduct at 350 nm, however, should only give rise to a photoion with an internal energy of between 21 and 36 kcal/mol, which would most likely be insufficient to permit prompt loss of any more than one additional CO ligand.

We must also allow for some mechanism for production of cluster-bound $Cr(CO)_6^+$ and $Cr(CO)_5^+$ ions in the 248-nm MPI scheme, although we have omitted these additional steps for the sake of clarity. Direct two-photon ionization of the sol

vated $Cr(CO)_6$ should yield a nascent ion having as much as 60 kcal/mol. This ion probably has sufficient internal energy to undergo prompt loss of one additional lig-

and, giving rise to a cluster-bound $Cr(CO)_5^+$ daughter ion in a manner analogous to that shown in the other two schemes.

Intracluster Energy Transfer. If the internal energies of the nascent photoproduct ions can be efficiently relaxed by transfer to an adjacent solvent molecule within the cluster, denoted as S in the schemes above, the extent to which the ions undergo loss of additional ligands via unimolecular decay will be somewhat reduced. It appears that CD_3OD is generally a more efficient acceptor of internal energy transferred from the nascent photoions. 248-nm MPI of CD_3OD-containing heteroclusters appears to be accompanied by a lesser degree of fragmentation of nascent, cluster-bound $Cr(CO)_6^+$ (and consequently lower yields of the $Cr(CO)_5^+$ daughter fragment), as well as less extensive fragmentation of the nascent $Cr(CO)_4^+$ (and consequently higher yields of the less unsaturated daughter, $Cr(CO)_3^+$). 350-nm MPI of CD_3OD-containing clusters proceeds with a lesser degree of fragmentation of the nascent cluster-bound $Cr(CO)_5^+$ (and consequently no detectable yield of the $Cr(CO)_4^+$ daughter). This observed isotope (or isotopomer) effect may be a consequence of non-statistical, mode-specific intracluster energy transfer between excited chromium carbonyl ions and adjacent solvent molecules within the van der Waals cluster. CD_3OD may be a more efficient acceptor molecule than CH_3OH because of fortuitous overlaps with the vibrational frequencies and symmetries of the various metal carbonyl species.

Conclusions

We have examined the multiphoton dissociation and ionization dynamics of van der Waals heteroclusters of $Cr(CO)_6$ and methanol generated in a pulsed free-jet expansion of seeded helium. We find that the multiphoton photophysics of $Cr(CO)_6$ solvated within van der Waals clusters is strikingly different from that of the naked molecule in the gas phase, in that molecular photoionization prevails over complete ligand stripping. We observe two principal series of cluster ions following 248-nm irradiation at moderate laser fluence (10^7 W/cm^2): a minor series corresponding to $S_nCr(CO)_x^+$ (x=5,6); and a major series corresponding to $S_nCr(CO)_x^+$ (x=0,1,2). We note that fragmentation is much more extensive under conditions of extremely high fluence (10^{12} to 10^{13} W/cm^2), and that fragmentation branching ratios are highly wavelength dependent. At 248 nm, irradiation at extremely high fluence leads to the appearance of the series, $S_nCr(CO)_x^+$ (x=0,1,2); while at 350 nm, the series corresponding to $S_nCr(CO)_xH^+$ (x=4,5) appears. At high fluence, evidence of extensive intracluster ion-molecule chemistry (i.e., proton transfer reactions, and solvent-solvent reactions leading to production of cluster-bound water) is observed. For all fluences, solvation by CD_3OD correlates with a less extensive degree of cluster ion photofragmentation than solvation by CH_3OH. The observation of a strong wavelength dependence in the

fluence regime where virtually all one-photon processes are expected to be saturated suggests either that a certain degree of wavelength-dependent photodissociative ligand loss precedes cluster ionization, or that cluster ion photofragmentation is not correctly described by a statistical model. We suggest that wavelength-dependent, one-photon photodissociation of the solvated $Cr(CO)_6$ takes place initially in the neutral manifold, and that the cluster-bound primary one-photon photoproduct subsequently undergoes MPI. Furthermore, we propose that the dependence of the extent of photoion fragmentation on the isotopomeric identity of the solvent can be accounted for in terms of a dynamical scheme involving mode-specific, intracluster energy transfer. CD_3OD appears to be more efficient than CH_3OH in its ability to accommodate the energy transferred from internal modes of the nascent metal carbonyl photoion.

Acknowledgment

We gratefully acknowledge the financial support of this work provided by the Office of Naval Research. JFG also acknowledges the Alfred P. Soan Foundation for a Research Fellowship (1991-1993).

Literature Cited

(1) Levine, R. D.; Bernstein, R. B. *Molecular Reaction Dynamics and Chemical Reactivity*; Oxford University Press: New York, NY, 1987.
(2) *Resonances in Electron Molecule Scattering, van der Waals Complexes, and Reactive Chemical Dynamics*; Truhlar, D. G., Ed.; ACS Symp. Series No. 263; American Chemical Society: Washington, D. C., 1984.
(3) Oxtoby, D. W. *J. Phys. Chem.* **1990**, *87*, 3028.
(4) Castleman, A. W., Jr.; Keesee, R. G. *Annu. Rev. Phys. Chem.* **1986**, *37*, 525.
(5) Echt, O.; Morgan, S.; Dao, P. D.; Stanley, R. J.; Castleman, A. W., Jr. *Ber. Bunsenges. Phys. Chem.* **1984**, *88*, 217.
(6) Wei, S.; Shi, Z.; Castleman, A. W., Jr. *J. Chem. Phys.* **1991**, *94*, 3268.
(7) Even, U.; Amirav, A.; Leutwyler, S.; Ondrechen, M. J.; Berkovitch-Yellin, Z.; Jortner, J. *Faraday Discuss. Chem. Soc.* **1982**, *73*, 153.
(8) Peifer, W. R.; Garvey, J. F. *J. Phys. Chem.* **1991**, *95*, 1177.
(9) Peifer, W. R.; Garvey, J. F. *J. Chem. Phys.* **1991**, *94*, 4821.
(10) Hoffmann, R. *Angew. Chem., Intl. Ed. Engl.* **1982**, *21*, 711.
(11) Meyer, T. J.; Caspar, J. V. *Chem. Rev.* **1985**, *85*, 187.
(12) Poliakoff, M.; Weitz, E. *Adv. Organomet. Chem.* **1986**, *25*, 277.
(13) Geoffroy, G. L.; Wrighton, M. S. *Organometallic Photochemistry*; Academic: New York, NY, 1979.
(14) Perutz, R. N.; Turner, J. J. *J. Am. Chem. Soc.* **1975**, *97*, 4800.

(15) Nathanson, G.; Gitlin, B.; Rosan, A. M.; Yardley, J. T. *J. Chem. Phys.* **1981**, *74*, 361.
(16) Yardley, J. T.; Gitlin, B.; Nathanson, G.; Rosan, A. M. *J. Chem. Phys.* **1981**, *74*, 370.
(17) Tumas, W.; Gitlin, B.; Rosan, A. M.; Yardley, J. T. *J. Am. Chem. Soc.* **1982**, *104*, 55.
(18) Hollingsworth, W. E.; Vaida, V. *J. Phys. Chem.* **1986**, *90*, 1235.
(19) Ouderkirk, A.; Weitz, E. *J. Chem. Phys.* **1983**, *79*, 1089.
(20) Ouderkirk, A.; Wemer, P.; Schultz, N. L.; Weitz, E. *J. Am. Chem. Soc.* **1983**, *105*, 3354.
(21) Seder, T. A.; Church, S. P.; Ouderkirk, A. J.; Weitz, E. *J. Am. Chem. Soc.* **1985**, *107*, 1432.
(22) Seder, T. A.; Church, S. P.; Weitz, E. *J. Am. Chem. Soc.* **1986**, *108*, 4721.
(23) Fletcher, T. R.; Rosenfeld, R. N. *J. Am. Chem. Soc.* **1983**, *105*, 6358.
(24) Holland, J. P.; Rosenfeld, R. N. *J. Chem. Phys.* **1988**, *89*, 7217.
(25) Ganske, J. A.; Rosenfeld, R. N. *J. Phys. Chem.* **1989**, *93*, 1959.
(26) Ishikawa, Y.; Brown, C. E.; Hackett, P. A.; Rayner, D. M. *J. Phys. Chem.* **1990**, *94*, 2404, and references therein.
(27) Joly, A. G.; Nelson, K. A. *J. Phys. Chem.* **1989**, *93*, 2876.
(28) Lee, M.; Harris, C. B. *J. Am. Chem. Soc.* **1989**, *111*, 8963.
(29) Simon, J. D.; Xie, X. *J. Phys. Chem.* **1986**, *90*, 6751.
(30) Simon, J. D.; Xie, X. *J. Phys. Chem.* **1989**, *93*, 291.
(31) Simon, J. D.; Xie, X. *J. Phys. Chem.* **1989**, *93*, 4401.
(32) Xie, X.; Simon, J. D. *J. Am. Chem. Soc.* **1990**, *112*, 1130.
(33) Wang, L.; Zhu, X.; Spears, K. G. *J. Am. Chem. Soc.* **1988**, *110*, 8695.
(34) Wang, L.; Zhu, X.; Spears, K. G. *J. Phys. Chem.* **1989**, *93*, 2.
(35) Moore, J. N.; Hansen, P. A.; Hochstrasser, R. M. *J. Am. Chem. Soc.* **1989**, *111*, 4563, and references therein.
(36) Yu, S.-C.; Xu, X.; Lingle, R., Jr.; Hopkins, J. B. *J. Am. Chem. Soc.* **1990**, *112*, 3668.
(37) Peifer, W. R.; Garvey, J. F. *J. Phys. Chem.* **1989**, *93*, 5906.
(38) Peifer, W. R.; Garvey, J. F. *Int. J. Mass Spectrom. Ion Proc.* **1990**, *102*, 1.
(39) Dearden, D. V.; Hayashibara, K.; Beauchamp, J. L.; Kirchner, N. J.; van Koppen, P. A. M.; Bowers, M. T. *J. Am. Chem. Soc.* **1989**, *111*, 2401.
(40) Hay, P. J. *J. Am. Chem. Soc.* **1978**, *100*, 2411.
(41) Fletcher, T. R.; Rosenfeld, R. N. *J. Am. Chem. Soc.* **1985**, *107*, 2203.
(42) Fletcher, T. R.; Rosenfeld, R. N. *J. Am. Chem. Soc.* **1988**, *110*, 2097.
(43) Bernstein, R. B. *J. Phys. Chem.* **1982**, *86*, 1178.
(44) Tyndall, G. W.; Jackson, R. L. *J. Chem. Phys.* **1989**, *91*, 2881.

Figure Captions

Figure 1) Mildly focused 248nm. MPI mass spectra of $Cr(CO)_6/CH_3OH$ heteroclusters where S=CH_3OH and the numbers above the bar represent n (reproduced with permission from ref. 9 copyright 1991 American Institute of Physics).

Figure 2) Mildly focused 248nm. MPI mass spectra of $Cr(CO)_6/CD_3OD$ heteroclusters where S=CD_3OD and the numbers above the bar represent n (reproduced with permission from ref. 9 copyright 1991 American Institute of Physics).

Figure 3a) Tightly focused 248nm. MPI mass spectra of $Cr(CO)_6/CH_3OH$ heteroclusters where S=CH_3OH and the numbers above the bar represent n.
Figure 3b) Tightly focused 248nm. MPI mass spectra of $Cr(CO)_6/CD_3OD$ heteroclusters where S=CD_3OD and the numbers above the bar represent n.

Figure 4a) Tightly focused 350nm. MPI mass spectra of $Cr(CO)_6/CH_3OH$ heteroclusters where S=CH_3OH and the numbers above the bar represent n.
Figure 4b) Expanded portion of 4a

Figure 5a) Tightly focused 350nm. MPI mass spectra of $Cr(CO)_6/CD_3OD$ heteroclusters where S=CD_3OD and the numbers above the bar represent n.
Figure 5b) Expanded portion of 5a
Figure 5c) Expanded portion of tightly focused 360nm. MPI mass spectra of $Cr(CO)_6/CD_3OD$ heteroclusters where S=CD_3OD and the numbers above the bar represent n.

Figure 6) Resonance enhanced MPI spectra of $Cr(CO)_6/CH_3OH$ heteroclusters. a) $Cr(CO)_5D^+$ signal vs laser wavelength produced following MPI of the $Cr(CO)_6/CD_3OD$ cluster beam. b) Cr^+ signal vs laser wavelength, produced following MPI of the $Cr(CO)_6/CH_3OH$ cluster beam. c) $(CH_3OH)_7H^+$ signal vs laser wavelength produced following MPI of the $Cr(CO)_6/CH_3OH$ cluster beam. d) Experimentally measured dye laser intensity vs wavelength.

FIGURE 1

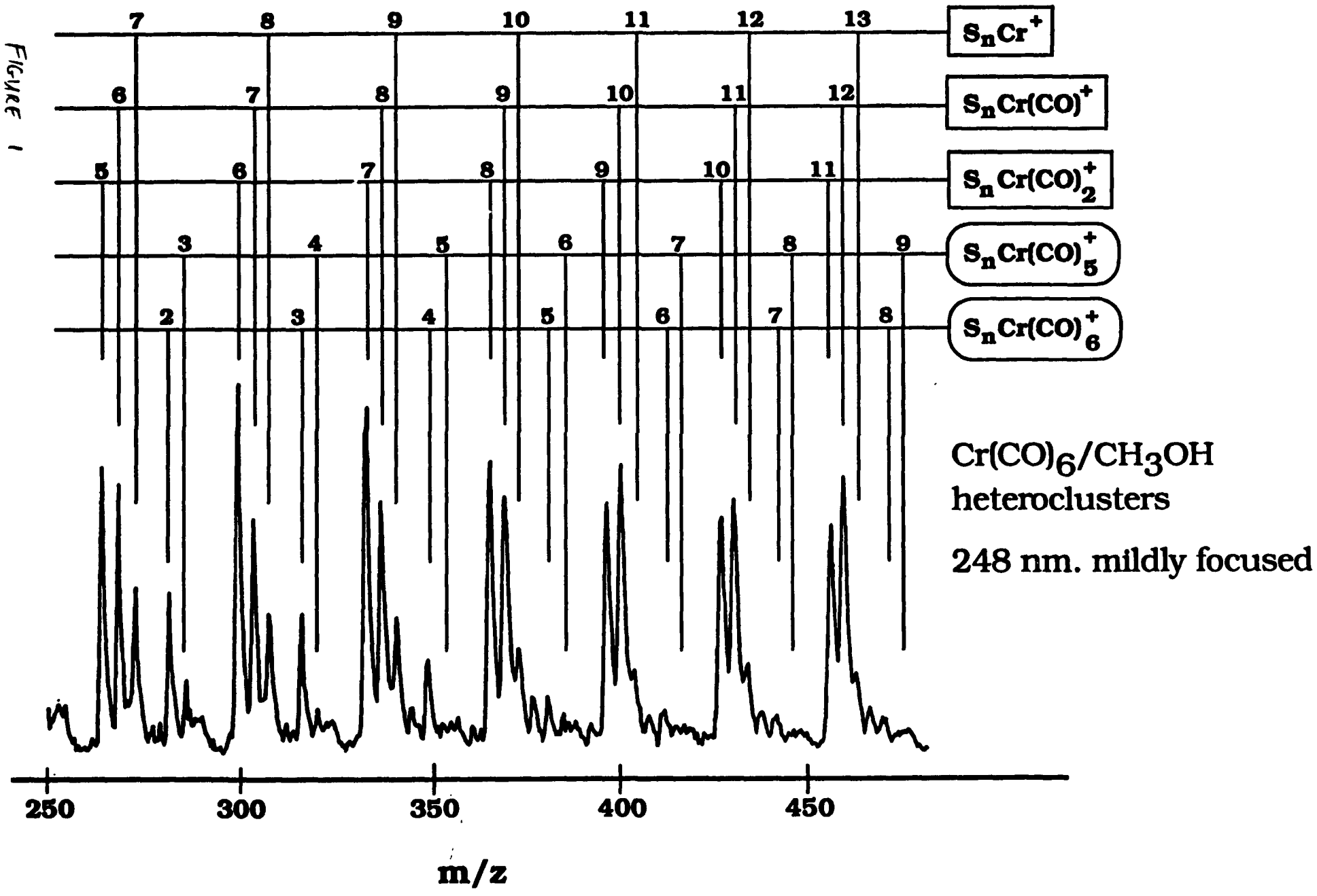

$Cr(CO)_6/CH_3OH$ heteroclusters

248 nm. mildly focused

FIGURE 2

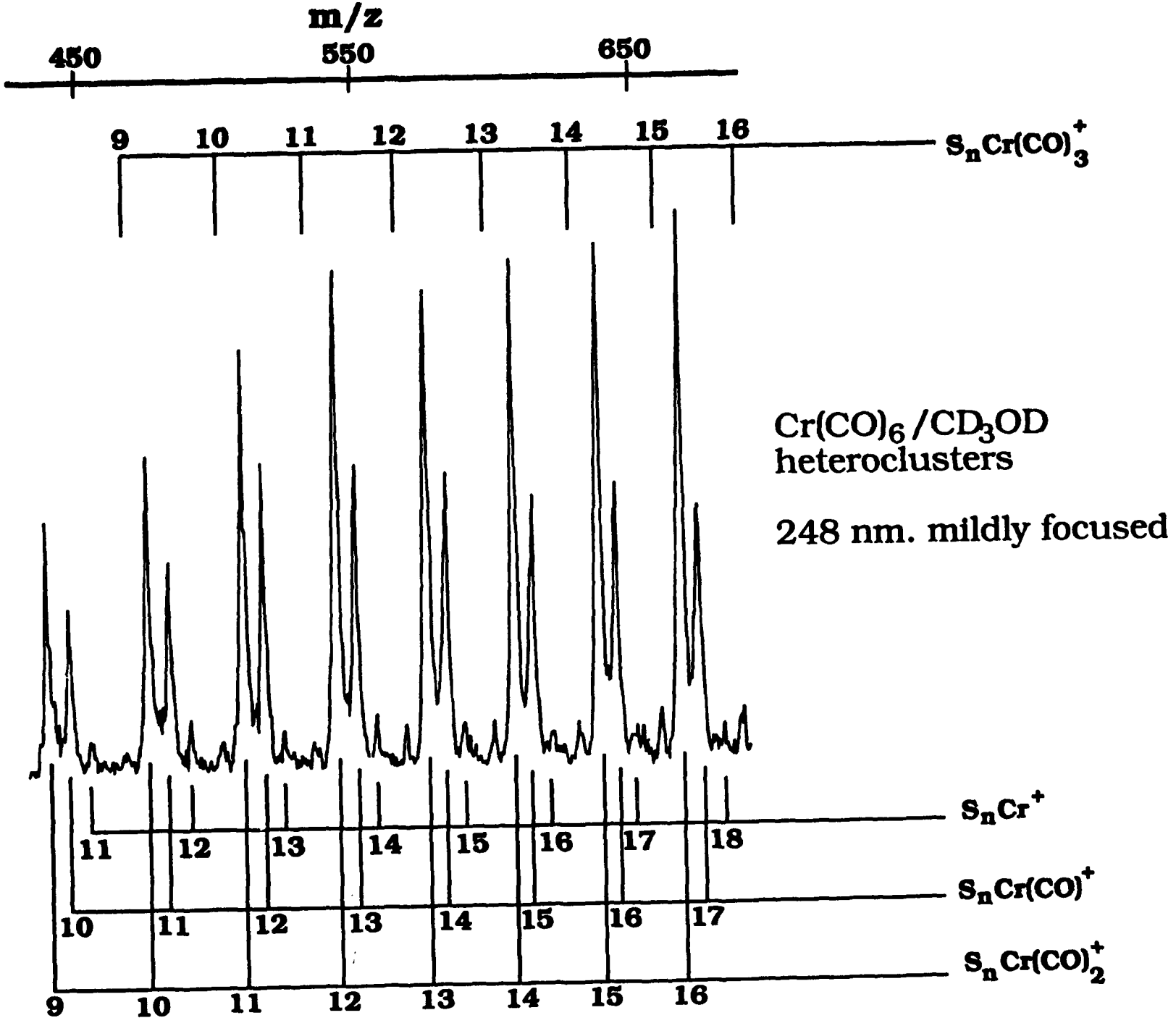
m/z
450
550
650
9 10 11 12 13 14 15 16
$S_nCr(CO)_3^+$
$Cr(CO)_6/CD_3OD$
heteroclusters
248 nm. mildly focused
S_nCr^+
11 12 13 14 15 16 17 18
$S_nCr(CO)^+$
10 11 12 13 14 15 16 17
$S_nCr(CO)_2^+$
9 10 11 12 13 14 15 16

Figure 34

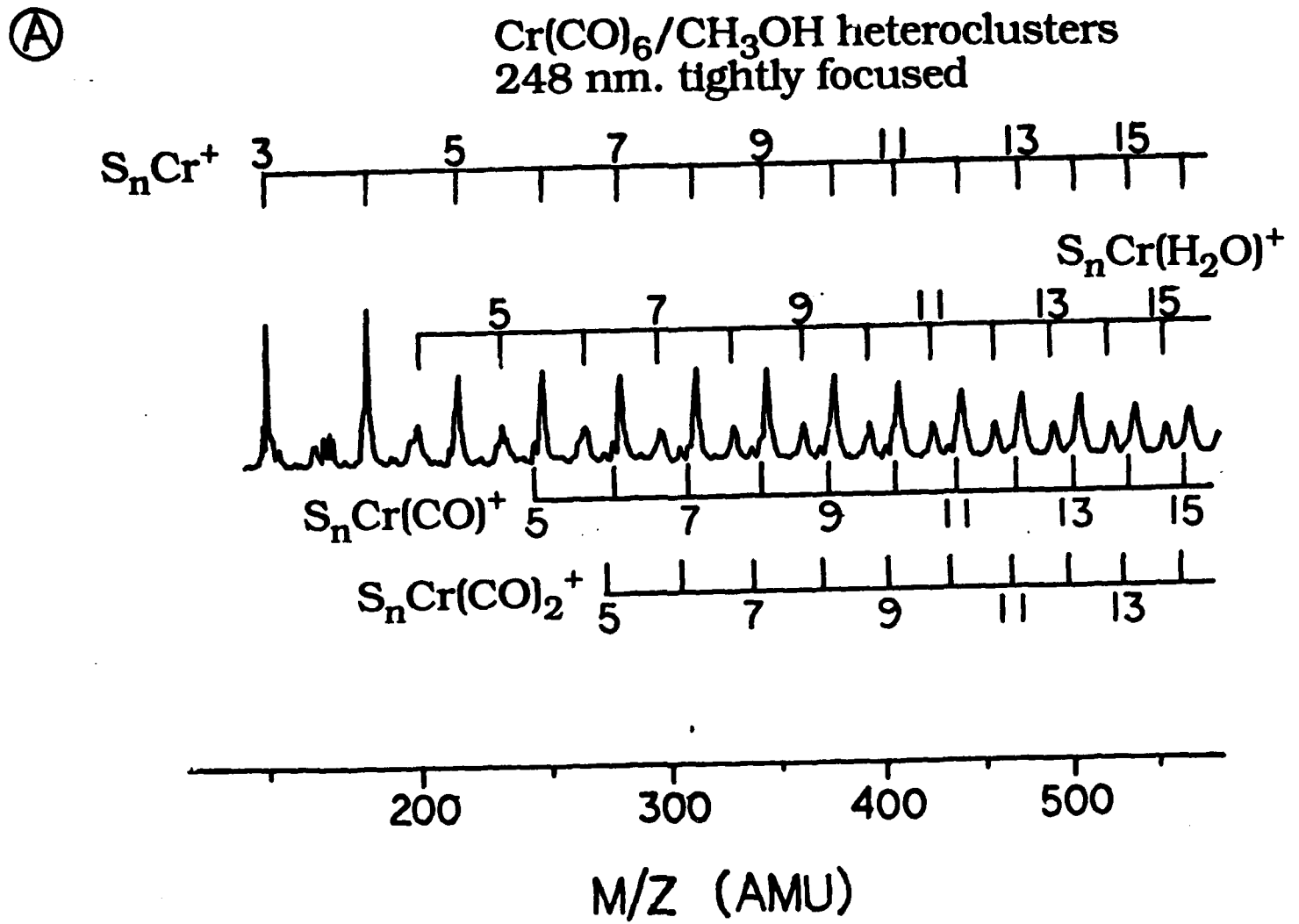
Ⓐ
Cr(CO)6/CH3OH heteroclusters
248 nm. tightly focused
SnCr+
3
5
7
9
11
13
15
SnCr(H2O)+
5
7
9
11
13
15
SnCr(CO)+
5
7
9
11
13
15
SnCr(CO)2+
5
7
9
11
13
200
300
400
500
M/Z (AMU)

Figure 3B

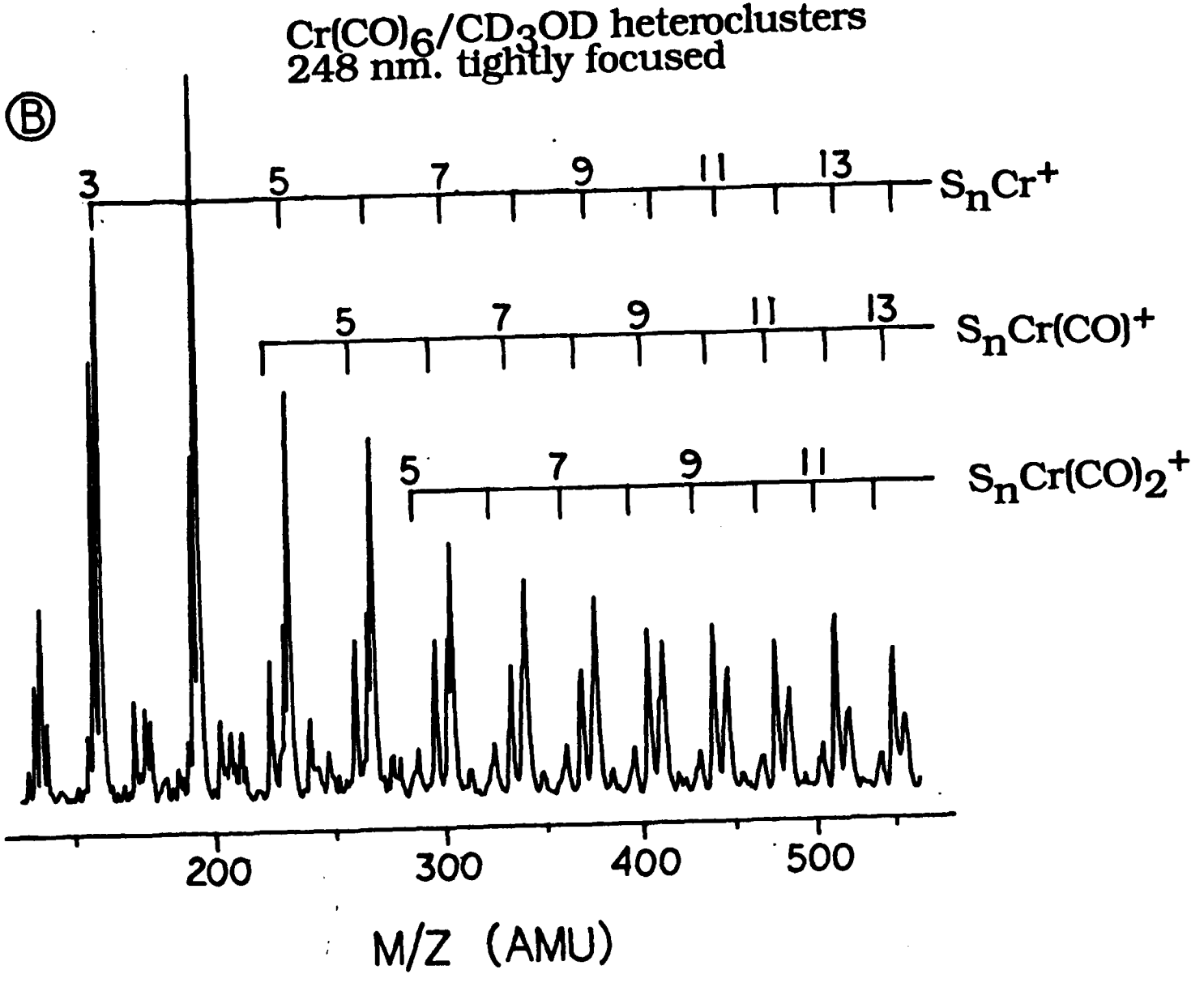
Cr(CO)6/CD3OD heteroclusters
248 nm. tightly focused
B
3
5
7
9
11
13
SnCr+
5
7
9
11
13
SnCr(CO)+
5
7
9
11
SnCr(CO)2+
200
300
400
500
M/Z (AMU)

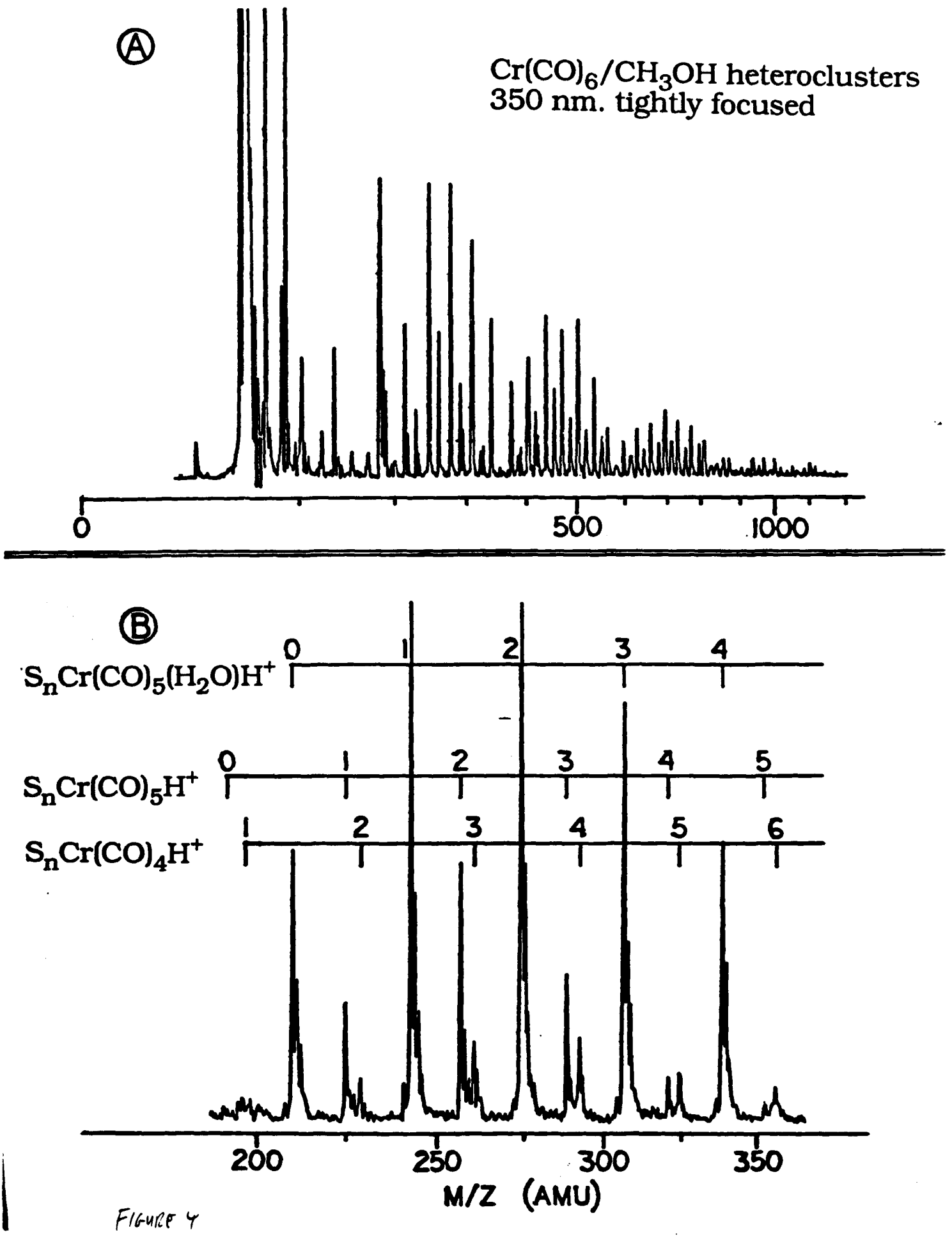
A
$Cr(CO)_6/CH_3OH$ heteroclusters
350 nm. tightly focused
0
500
1000
B
$S_nCr(CO)_5(H_2O)H^+$
$S_nCr(CO)_5H^+$
$S_nCr(CO)_4H^+$
0
1
2
3
4
5
6
200
250
300
350
M/Z (AMU)

FIGURE 4

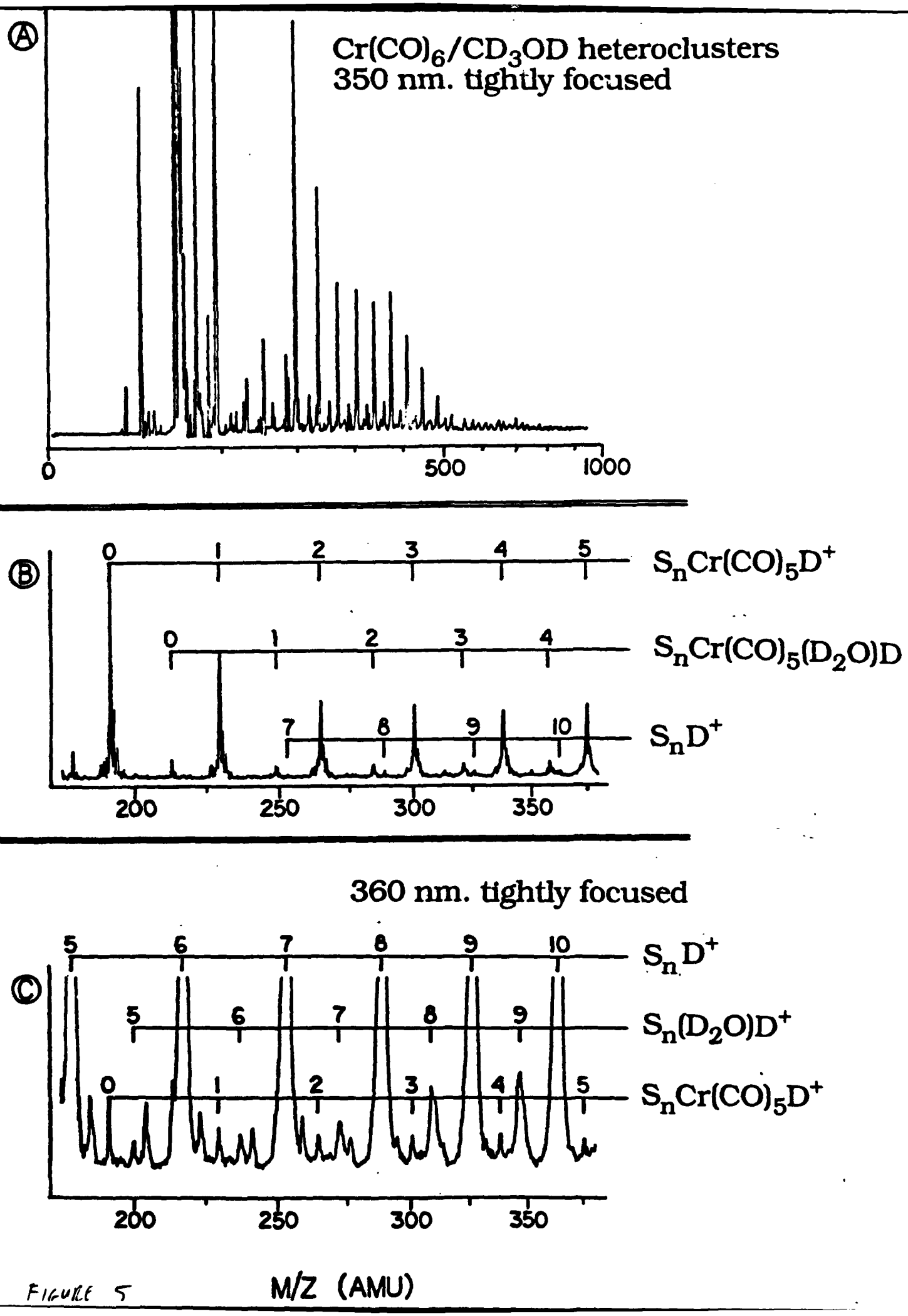
A
Cr(CO)6/CD3OD heteroclusters
350 nm. tightly focused
0
500
1000
B
0 1 2 3 4 5
SnCr(CO)5D+
0 1 2 3 4
SnCr(CO)5(D2O)D
7 8 9 10
SnD+
200
250
300
350
360 nm. tightly focused
C
5 6 7 8 9 10
SnD+
5 6 7 8 9
Sn(D2O)D+
0 1 2 3 4 5
SnCr(CO)5D+
200
250
300
350
M/Z (AMU)

FIGURE 5

REMPI spectra

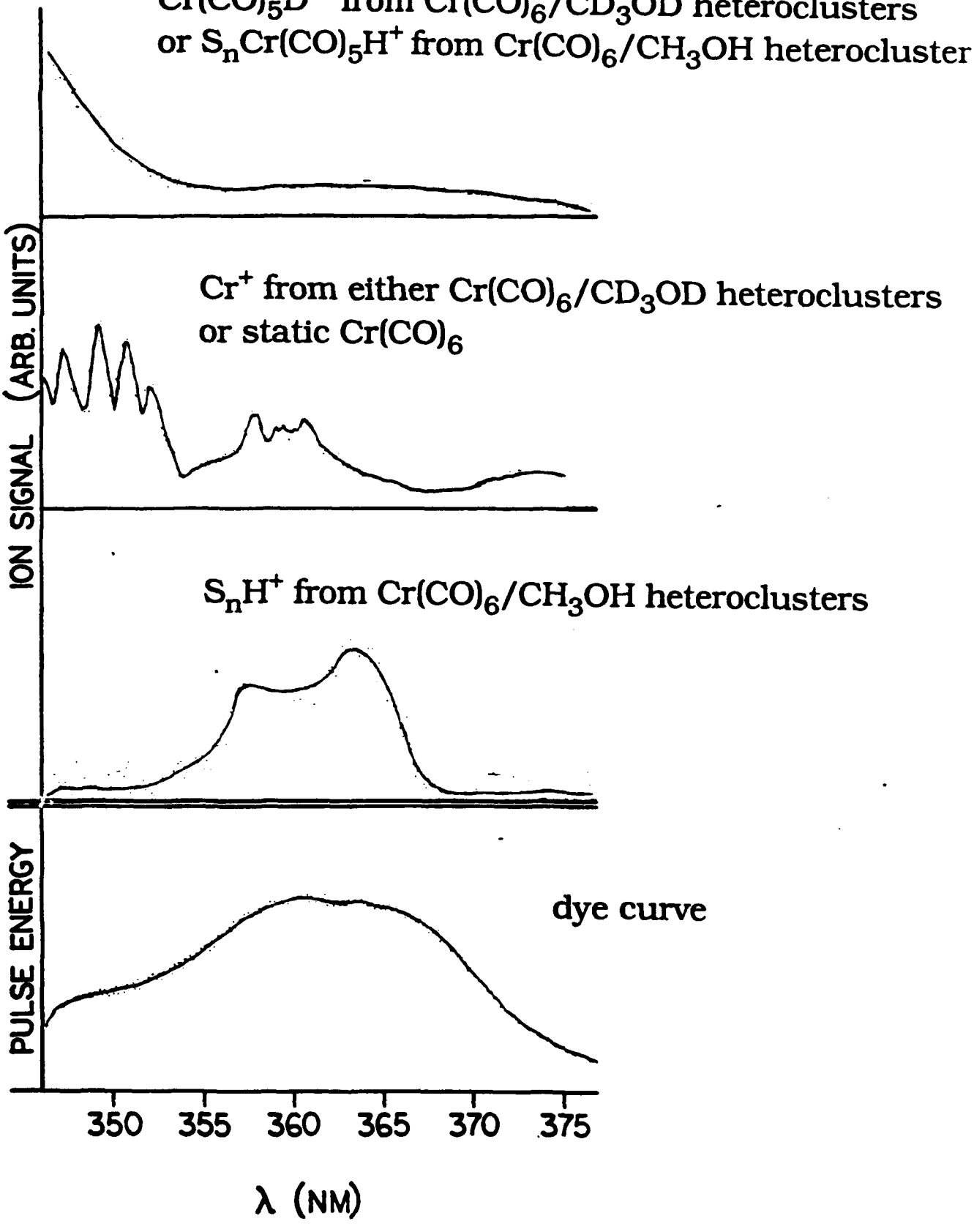

FIGURE 6